XVI IMEKO World Congress
Measurement - Supports Science - Improves Technology - Protects Environment ... and Provides Employment - Now and in the Future
Vienna, AUSTRIA, 2000, September 25-28

CONTACT FORCE AND POSITION SENSOR WITH QUARTZ RESONATORS

S. Muraoka
Osaka Institute of Technology
5-16-1, Ohmiya, Asahi-ku, Osaka 535-8585, Japan

Abstract: Because it is superior in local sensing, tactile sensing for environment recognition has been studied. In this paper, a contact force and position sensor for recognizing the environment and controlling the grasp force is proposed. The sensor incorporates four pairs of quartz resonators mounted in a robot finger and can measure two-dimensional contact force and one-dimensional contact position along the finger. The force sensor is insensitive to electrical noise since the output is a frequency which shifts in response to a change in the external force. This type of force sensor also has quick response, high sensitivity, high resolution and wide bandwidth. The performance of the sensor was examined experimentally. To demonstrate the capabilities of the sensor in recognizing an environment, two-dimensional shapes were reconstructed by tracing the surface with the sensor.
Keywords: sensor, quartz resonator, contact force and position

1 INTRODUCTION

Because it is superior in local sensing, tactile sensing for environment recognition has been studied. In this paper, a contact force and position sensor for recognizing the environment and controlling the grasp force is proposed. The sensor incorporates four pairs of quartz resonators mounted in a robot finger and can measure two-dimensional contact force and one-dimensional contact position along the finger.

Many force sensors used in robots utilise strain gauges. These force sensors are readily affected by electrical noise, and often require amplifiers, filters and A-D converters because their output is analogue and of a low level. However, a force sensor using quartz resonators is insensitive to electrical noise because its output is a frequency. The output frequency can easily be converted into a digital signal through a frequency counter. In addition, the output of the frequency counter can be directly connected to a computer without an A-D converter. The force sensor also has quick response, high sensitivity and high Resolution Furthermore, since the frequency of a quartz resonator is generally much higher than the frequency of environmental noise, the sensor can have a wide bandwidth even when use with filters. Therefore, it could be used in an environment with a noisy Background and in cases requiring a quick response.

Although force sensors using quartz resonators have many advantages, such as those mentioned above, such sensors have not yet been applied in measuring dynamic quantities such as contact force and contact position. The sensor proposed here can measure such dynamic quantities. Unusual events in the quartz resonators can be monitored and the finger can still be used even when one pair of the resonators is damaged. In this paper, I call this sensor the contact force and position sensor. The performance of the sensor was examined experimentally. As a demonstration of the sensors ability to recognize an environment, a half disk and a semicircular hole were reconstructed by tracing the surface of the environment with the sensor.

2 A SENSOR FOR MFASURING CONTACT FORCE AND CONTACT POSITION

2.1 Structure and principle of the sensor

AT-cut quartz resonators of thickness D = 0.17 mm width W= 8 mm and length L = 10 mm were used in the experiments. The fundamental frequency was 10 ± 0.05 MHz, and the mode of vibration was a thickness shear mode. An external force was applied at y = 35 ± 1 °C to the electric-axis of the quartz resonator, where the force sensitivity is independent of temperature [1]. An experimental finger with four pairs of quartz resonators was made.

The finger functioned as a contact force and position sensor, and was fixed on a triangular test stand. An external force was applied at an angle *q* to the Y-axis as shown in Fig. 1. Eight grooves were machined by spark erosion at symmetrical positions relative to the neutral plane of the finger. The dimensions of the grooves were 0.2 mm in width and 1 mm in depth. Both ends of each quartz resonator were inserted into the grooves and glued to the finger with cyano-acrylate adhesive. The differential method [2] was applied to reduce the influence of an external disturbance. The X-axis lies along the major axis of the finger, while the Y-axis is in the direction of movement of the finger, and the Z-axis makes up the Cartesian frame. 1 chose the origin to be at the fixed end of the finger. Referring to Fig. 1, the force *F* acts at the point P in the *Y-Z* plane. F_y and F_z are the components of *F* in the *Y* and *Z* directions, respectively, 0 is the angle between the direction of *F* and the Y-axis and X is the X co-ordinate of point P.

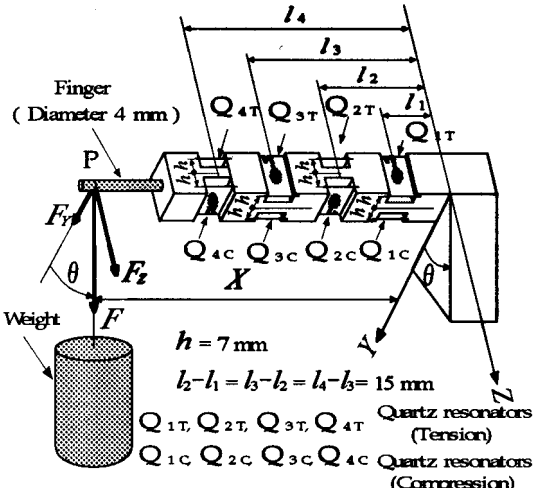

Figure 1. A finger as a contact force and position sensor with four pairs of quartz resonators fixed on the test stand

The quartz resonators are referred to by symbol Q, and the subscripts 1, 2, 3 and 4 are attached to the symbols depending on the resonator's position from the fixed end of the finger. The subscripts T and C are attached to the symbols depending on whether the resonators are subjected to tension or compression, respectively. The difference in the frequency shifts for each pair of quartz resoriators is expressed as Out_1~ Out_4 (Q_{1T} and Q_{1C} ~ Q_{4T} and Q_{4C}). The position of each pair of resonators from the fixed end of the finger is denoted by l_1 ~ l_4 and the distance between each resonator and the neutral planes of the finger is denoted by *h.* The moment of inertia about the neutral axis at the areas where the quartz resonators are mounted is denoted by *I*. The mean normal stresses of the individual resonators (s_{1T} *and* s_{1C}) ~ (s_{4T} *and* s_{4C}) are given by

$$\sigma_{1T} = -\sigma_{1C} = F_Y (X-l_1)\, h / I = (X-l_1)\, h F \cos\theta / I \quad (1)$$
$$\sigma_{2T} = -\sigma_{2C} = F_Z (X-l_2)\, h / I = (X-l_2)\, h F \sin\theta / I \quad (2)$$
$$\sigma_{3T} = -\sigma_{3C} = F_Y (X-l_3)\, h / I = (X-l_3)\, h F \cos\theta / I \quad (3)$$
$$\sigma_{4T} = -\sigma_{4C} = F_Y (X-l_4)\, h / I = (X-l_4)\, h F \sin\theta / I \quad (4)$$

The difference in the frequency shifts *Out* is as follows [3].

$$Out = (f_C - f_T) - (f_{0C} - f_{0T})$$
$$= [(f_{0C} + f_{0T})\,\mu_0 + (f_{0C}\cos 2\psi_C + f_{0T}\cos 2\psi_T)\,\mu_1 + \{(f_{0C} + f_{0T})\,\nu_0 + (f_{0C}\cos 2\psi_C + f_{0T}\cos 2\psi_T)\,\nu_1\}\,T]\,\sigma \quad (5)$$

where f_0 and *f* denote the frequencies when *F* = 0 and *F* 0, respectively, *T* is the temperature in centigrade, and μ_0=14.1x10^{-12} Pa^{-1}, μ_1=13.1x10^{-12} Pa^{-1}, ν_0=-9.9x10^{-15} Pa^{-1} K^{-1} and ν_1=28.4x10^{-15} Pa^{-1}K^{-1} [1]. When the force directions $\varnothing_C$ and $\varnothing_T$ to the electric-axis of a quartz resonator are selected so as to satisfy the relationship

$$f_{0C}\cos 2\psi_C + f_{0T}\cos 2\psi_T = -(f_{0C}+f_{0T})\,\nu_0 / \nu_1 \quad (6)$$

Eq.(5) becomes as follows.

$$Out = (f_0+f_{0T})\,\{\mu_0 - \mu_1 (\nu_0/\nu_1)\}\,\sigma_T \quad (7)$$

Eq. (7) means that *Out* is independent of temperature T. In the experiments carried out and the following discussion, I assume that the condition of Eq. (6) is satisfied because the quartz resonators are mounted to the finger with $\varnothing_C$ and $\varnothing_T$ equal to 35°. The differences of frequency shifts are, according to eqs. (7) and (1) ~ (4), given by

$$Out_1 = A_1\gamma (X - l_1) F_Y = A_1\gamma (X - l_1) F \cos\theta \quad (8)$$
$$Out_2 = A_2\gamma (X - l_2) F_Z = A_2\gamma (X - l_2) F \sin\theta \quad (9)$$
$$Out_3 = A_3\gamma (X - l_3) F_Y = A_3\gamma (X - l_3) F \cos\theta \quad (10)$$
$$Out_4 = A_4\gamma (X - l_4) F_Z = A_4\gamma (X - l_4) F \sin\theta \quad (11)$$

where

$$A_1 = f_{01C} + f_{01T}, \quad A_2 = f_{02C} + f_{02T}, \quad A_3 = f_{03C} + f_{03T}, \quad A_4 = f_{04C} + f_{04T}, \quad \gamma = \{\mu_0 - \mu_1 (\nu_0/\nu_1)\}\, h / I \quad (12)$$

Two components, F_v and F_z, of contact force and the co-ordinate, X, of the contact point P are, according to eq. (8) ~ (11), given by

$$F_Y = (A_3 Out_1 - A_1 Out_3) / \{A_1 A_3 \gamma (\ell_3 - \ell_1)\} \quad (13)$$
$$= Out_3 (A_4 Out_2 - A_2 Out_4) / [A_3 \gamma \{A_4 (\ell_4 - \ell_3) Out_2 + A_2 (\ell_3 - \ell_2) Out_4\}] \quad (14)$$
$$= Out_1 (A_2 Out_4 - A_4 Out_2) / [A_1 \gamma \{A_2 (\ell_2 - \ell_1) Out_4 + A_4 (\ell_1 - \ell_4) Out_2\}] \quad (15)$$

$$F_Z = (A_4 Out_2 - A_2 Out_4) / \{A_2 A_4 \gamma (\ell_4 - \ell_2)\} \quad (16)$$
$$= Out_2 (A_3 Out_1 - A_1 Out_3) / [A_2 \gamma \{A_3 (\ell_3 - \ell_2) Out_1 + A_1 (\ell_2 - \ell_1) Out_3\}] \quad (17)$$
$$= Out_4 (A_3 Out_1 - A_1 Out_3) / [A_4 \gamma \{A_3 (\ell_3 - \ell_4) Out_1 + A_1 (\ell_2 - \ell_1) Out_3\}] \quad (18)$$

$$X = (A_3 \ell_3 Out_1 - A_1 \ell_1 Out_3) / (A_3 Out_1 - A_1 Out_3) \quad (19)$$
$$= (A_4 \ell_4 Out_2 - A_2 \ell_2 Out_4) / (A_4 Out_2 - A_2 Out_4) \quad (20)$$

The contact force F and its direction è are given by

$$F = (F_Y^2 + F_Z^2)^{1/2} \quad (21)$$
$$\theta = \tan^{-1} (F_Z / F_Y) \quad (22)$$

In eqs. (8)~(11), *Out_2 and Out_4* are 0 when the force direction è is 0°, and *Out_1 and Out_3* are 0 when è is 90°. F_v and F_z are obtained from eqs. (13) and (16) which do not have the variable *Out* in the denominator. X is obtained from eq. (19) except when è = 90°, and from eq. (20) except when è=0°. As shown in eqs. (13)~(20), F_v and F_z and X can also be obtained from any three of Out_1~Out_4.That is, they can be obtained from eqs. (13), (17) and (19) when the pairs of quartz resonators Q_1, Q_2 and Q_3 are used, from eqs. (14), (16) and (20) when Q_2, Q_3, and Q_4 are used, from eqs. (13), (18) and (19) when Q_3, Q_4 and Q_1 are used, and from eqs. (15), (16) and (20) when Q_4, Q_1 and Q_2 are used. Therefore, in a finger with four pairs of resonators, a plural output can be obtained simultaneously. This makes it possible to monitor an unusual event in one pair of quartz resonators. Thus, the sensor can function from the output of only three pairs of resonators when the output from one pair is unusual. Where three pairs only used, two of the quantities F_v and F_z and X cannot be obtained when the force direction è is 0° or 90°. The force sensitivity can be adjusted by varying the moment of inertia I, the mounted position h of the quartz resonators, and the distance l between each pair of quartz resonators.

2.2 Experimental performances of the sensor

An external force F was applied to the finger shown in Fig. 1 at angle è to the Y-axis. è was changed in increments of 15° in the range 0° to 90°. For each è, Out_1 ~ Out_4 were measured at (I) 0.98 N incremental steps in F in the range 0 ~ 4.9 N with X = 0.194 m, and (II) 0.01 m incremental steps in X in the range 0.164~0.224 m with F = 2.94 N. These experiments were carried out three times. The measurement system used for each pair of resonators is shown in Fig. 2.
Eqs. (8) ~ (11) are rewritten for individual pairs of quartz resonators in the form

$$Out_1 = k_{F1} F \quad Out_2 = k_{F2} F \quad Out_3 = k_{F3} F \quad Out_4 = k_{F4} F \quad (23)$$
$$Out_1 = k_{X1} X - \ell_{X1} \quad Out_2 = k_{X2} X - \ell_{X2} \quad Out_3 = k_{X3} X - \ell_{X3} \quad Out_4 = k_{X4} X - \ell_{X2} \quad (24)$$
$$Out_1 = k_{\theta 1} \cos\theta \quad Out_2 = k_{\theta 2} \sin\theta \quad Out_3 = k_{\theta 3} \cos\theta \quad Out_4 = k_{\theta 4} \sin\theta \quad (25)$$

where

$$k_{F1} = A_1 \gamma (X - \ell_1) \cos\theta \quad k_{F2} = A_2 \gamma (X - \ell_2) \sin\theta \quad k_{F3} = A_3 \gamma (X - \ell_3) \cos\theta \quad k_{F4} = A_4 \gamma (X - \ell_4) \sin\theta \quad (26)$$
$$k_{X1} = A_1 \gamma F \cos\theta \quad k_{X2} = A_2 \gamma F \sin\theta \quad k_{X3} = A_3 \gamma F \cos\theta \quad k_{X4} = A_4 \gamma XF \sin\theta$$
$$\ell_{X1} = A_1 \gamma \ell_1 F \cos\theta \quad \ell_{X2} = A_2 \gamma \ell_2 F \sin\theta \quad \ell_{X3} = A_3 \gamma \ell_3 F \cos\theta \quad \ell_{X4} = A_4 \gamma \ell_4 F \sin\theta \quad (27)$$
$$k_{\theta 1} = A_1 \gamma (X - \ell_1) F \quad k_{\theta 2} = A_2 \gamma (X - \ell_2) F \quad k_{\theta 3} = A_3 \gamma (X - \ell_3) F \quad k_{\theta 4} = A_4 \gamma (X - \ell_4) F \quad (28)$$

Eqs. (23) ~ (25) were verified experimentally. First, the linear regression in F of the measured values Out_1 ~ Out_4 gave the coefficients k_{F1} ~ k_{F4} from eq. (23). The standard deviations s_{F1} ~ s_{F4} were also obtained. These values are shown in Table 1 (A). Linear regression to obtain the coefficients k_{x1} ~ k_{x4} and l_{x1} – l_{x4} in eq. (24) and their standard deviations s_{x1} - s_x, was also done. These values are shown in Table 1 (B). Furthermore the coefficients $k_{è1}$ ~ $k_{è4}$ in eq. (25) and their standard deviations $s_{è1}$ ~ $s_{è4}$ were found using the same method. These values are shown in Table 1 (C). From the standard deviations the overall accuracy was estimated to be a few parts in a thousand considering that the Maximum value of the frequency shift produced by an external force may be several tens of kHz. Fig.

3 shows graphically the data shaded in Table 1. The symbols , •, ⋆ and x refer to the experimental values of Out_1, Out_2, Out_3 and Out_4 respectively, and the solid lines are regression lines. In Fig. 3, (A) shows the relationships between Out_1 ~ Out_4 and è when X=0.194 m and F=2.94 N. (B) shows the relationships between Out_1 ~ Out_4 and X when F= 2.94 N and è = 30°, and (C) and (D) show the relationships between Out_1 ~ Out_4 and F when è = 0° and è = 90°, demonstrating that the cross sensitivity can, in practice, be neglected. (E) and (F) show relationships between Out_1 ~ Out_4 and F when è = 30° and X=0.194 m, and when è=60° and X = 0.194 m, respectively.

Since A_1 A_2 A_3 $A4$ 20 MHz and $(l_2 - l_1) = (l_3 - l_2) = (l_4 - l_3) = 0.150$ mm in the experiments, eqs. (13) ~ (20) become

$$F_V \approx k_1\{Out_1 - Out_3\} \quad (29)$$
$$\approx k_2\{Out_3\,(Out_2-Out_4) / (Out_2+Out_4)\} \quad (30)$$
$$\approx k_3\{Out_1\,(Out_4-Out_2) / (Out_4-3Out_2)\} \quad (31)$$
$$F_Z \approx k_4\{Out_2 - Out_4\} \quad (32)$$
$$\approx k_5\{Out_2\,(Out_1-Out_3) / (Out_1+Out_3)\} \quad (33)$$
$$\approx k_6\{Out_4\,(Out_1-Out_3) / (3Out_3-Out_1)\} \quad (34)$$
$$X \approx k_7 + k_8\{Out_1 / (Out_1 - Out_3)\} \quad (35)$$
$$\approx k_9 + k_{10}\{Out_2 / (Out_2 - Out_4)\} \quad (36)$$

where k_1 ~ k_{10}, are coefficients. By substituting the measured values Out_1 ~ Out_4 into eqs. (29) ~ (36), the coefficients k_1~k_{10} are found by linear regression. Fig. 4 shows the relationships of eqs. (29)~(36). The vertical axes refer to the values given on the right hand sides of the equations derived from the coefficients and the measured values, and the horizontal axes are for the values set up in the experiments. The values on the right hand sides lie approximately on straight lines inclined at 45". This means that the values on the right hand sides agree with the set up values. (A) ~ (H) correspond to eqs. (29) ~ (36), respectively. The denominators shown in the ordinates of (B), (C) and (H) are 0 when è = 0°. In this case, the right hand sides of eqs. (27), (28) and (33) cannot be found. The denominators shown in the ordinates of (E), (F) and (G) are 0 when è=90°. In this case, the right hand sides of eqs. (30), (31) and (32) also cannot be found. Experimental values of these cases are not drawn in the figures. In (E), (F) and (G), the errors become large for small denominators when è is 75° (symbol o), i.e. near 90°. In (H), the errors become large for small denominators when è is 15° (symbol •) i.e. near 0°.

since a sensor is generally used after calibration, it is appropriate for the sensor to be evaluated by the results of the regression analysis. Thus, F_V and F_Z and X were derived by substituting measured values Out_1 ~ $0ut_4$ in eqs. (29) ~ (36). From this it was shown that the finger functions as a sensor for F_V and F_Z and X.

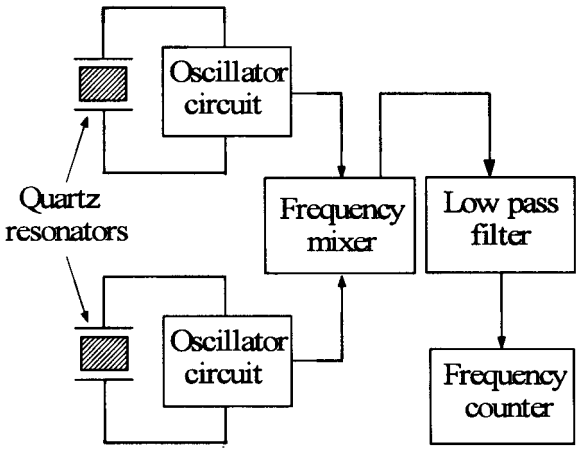

Figure 2. Block diagram of measurement system

Table 1. Out_1, Out_2, Out_3 and Out_4 with respect to (A) contact force F, (B) contact position X and (C) force direction è

(A)

X [m]	θ [°]	$Out_1=k_{F1}F$ k_{F1} [Hz/N]	s_{F1} [Hz]	$Out_2=k_{F2}F$ k_{F2} [Hz/N]	s_{F2} [Hz]	$Out_3=k_{F3}F$ k_{F3} [Hz/N]	s_{F3} [Hz]	$Out_4=k_{F4}F$ k_{F4} [Hz/N]	s_{F4} [Hz]
0.194	0	447.9	1.3	0.4	0.6	380.8	0.9	8.2	1.0
	15	429.8	1.1	101.2	2.3	366.9	0.6	85.5	1.7
	30	383.2	2.5	190.8	1.3	327.9	1.0	154.0	1.2
	45	314.0	1.6	268.3	2.8	268.9	0.6	212.9	1.9
	60	220.9	1.9	328.0	0.8	190.5	1.2	257.7	2.9
	75	115.0	0.5	365.2	1.5	100.4	0.8	283.8	1.1
	90	0.9	0.3	377.5	2.0	2.2	2.0	291.6	1.3

(B)

F [N]	θ [°]	$Out_1=k_{X1}X-l_{X1}$ k_{X1} [Hz/m]	l_{X1} [m]	s_{X1} [Hz]	$Out_2=k_{X2}X-l_{X2}$ k_{X2} [Hz/m]	l_{X2} [m]	s_{X2} [Hz]	$Out_3=k_{X3}X-l_{X3}$ k_{X3} [Hz/m]	l_{X3} [m]	s_{X3} [Hz]	$Out_4=k_{X4}X-l_{X4}$ k_{X4} [Hz/m]	l_{X4} [m]	s_{X4} [Hz]
2.94	0	8620	-358	2	10	4	0	9158	-658	5	81	7	2
	15	8339	-351	3	2089	-112	3	8873	-640	4	2142	-166	5
	30	7517	-319	2	4118	-239	2	7952	-569	4	4079	-338	3
	45	6155	-268	5	5745	-328	6	6424	-440	4	5758	-490	5
	60	4286	-179	2	7054	-403	4	4499	-310	1	6988	-597	2
	75	2338	-96	4	8112	-467	3	2335	-149	4	7848	-676	5
	90	100	-9	0	8138	-467	4	0	-2	1	8020	-695	2

(C)

X [m]	F [N]	$Out_1=k_{\theta1}\cos\theta$ $k_{\theta1}$ [Hz]	$s_{\theta1}$ [Hz]	$Out_2=k_{\theta2}\sin\theta$ $k_{\theta2}$ [Hz]	$s_{\theta2}$ [Hz]	$Out_3=k_{\theta3}\cos\theta$ $k_{\theta3}$ [Hz]	$s_{\theta3}$ [Hz]	$Out_4=k_{\theta4}\cos\theta$ $k_{\theta4}$ [Hz]	$s_{\theta4}$ [Hz]
0.194	0.98	437	2	367	4	369	0	277	5
	1.96	873	3	742	3	745	3	581	11
	2.94	1308	9	1113	5	1117	3	872	11
	3.92	1745	7	1484	6	1491	5	1162	22
	4.90	2190	16	1843	10	1849	8	1389	17

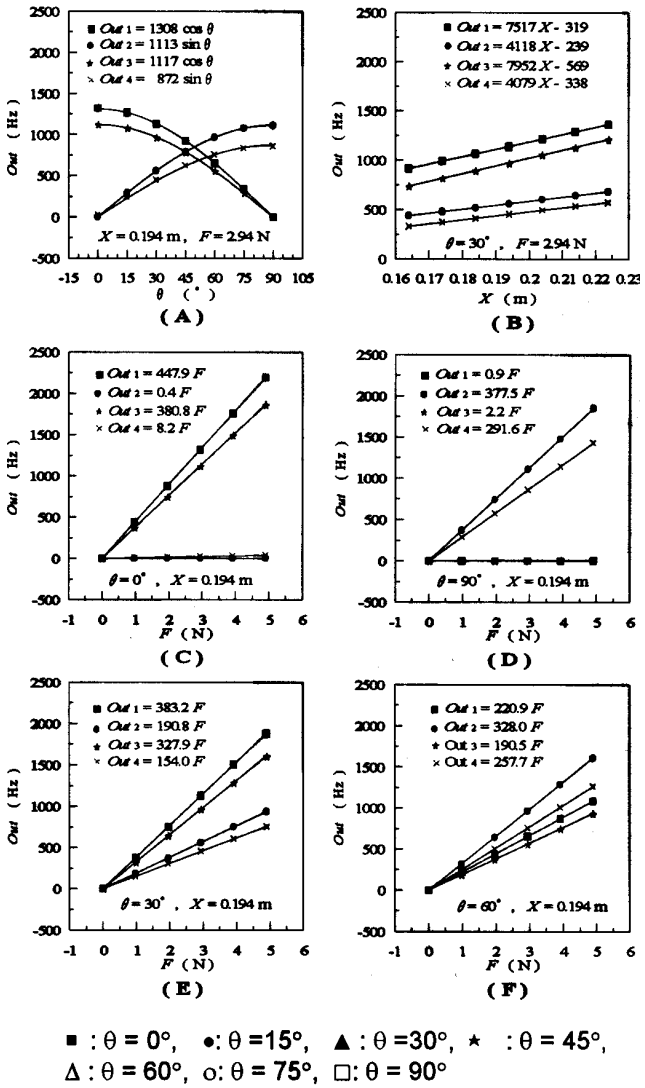

Figure 3. Out_1, Out_2, Out_3 and Out_4 with respect to (A) force direction è, (B) contact position X and (C) contact force F when è =0°, (D) F when è = 90°, (E) F when è = 30° and (F) F when è = 60°.

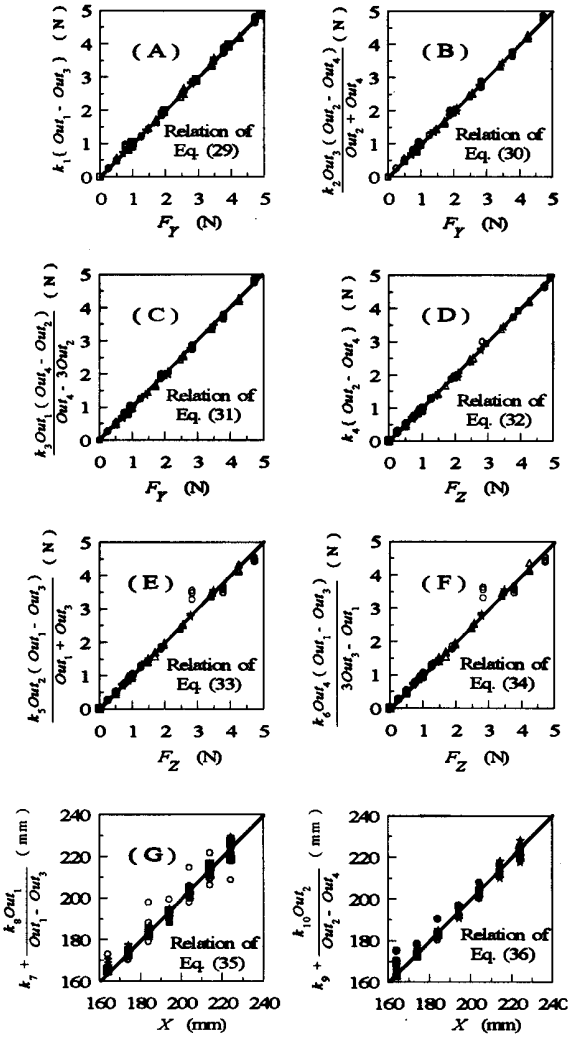

Figure 4. Relationship between measured values of F_y, F_z and X and their setup values

3 SENSING AN ENVIRONMENT

As shown in Fig 5, the environment was moved along the Z-axis and traced by the finger moving along the Y-axis. The finger fulfills function as a contact force and position sensor. Two motors to move the finger and the environment were controlled simultaneously so that contact force F was kept at 1 ± 0.1 N. The turning angles of the two motors give the coordinates (Y_f, Z_f) of the finger. F_v and F_z were obtained by substituting measured values of Out_1 ~ Out_4 in eqs. (29) and (32). The contact force F and its direction è were obtained by substituting F_v and F_z in eqs. (21) and (22). The two-dimensional shape of the environment corresponds to the locus of the contact point between the finger and the environment. Therefore, the shape could be

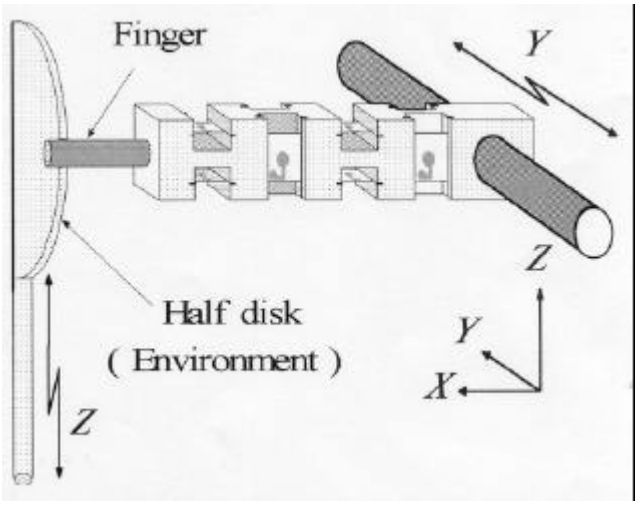

Figure 5. Experimental setup for sensing an environment

found by converting the locus of the finger to the locus of the contact point by using the following relations.

$$Y_e = Y_f - R\cos\theta \quad (37)$$
$$Z_e = Z_f - R\sin\theta \quad (38)$$

where Y_e and Z_e are the coordinates of the contact point, and R is radius of the finger. The two-dimensional shape of the environment was reconstructed by finding the locus of (Y_e, Z_e). The outer circumference of a half disk with radius 15 mm was reconstructed as shown in Fig. 6 (A). In the figure, (1) shows the locus of the finger which is larger than the disk by the radius R. The inner circumference of a semicircular hole with radius 15 mm was reconstructed as shown in Fig. 6 (B). In the figure, (1) shows the locus of the finger which is smaller than the hole by R. In (2) of (A) and (2) of (B), the locus of each two-dimensional shape (Y_e, Z_e) is shown. The locus (Y_e, Z_e) shown in (2) of (A) is a little smaller than the disk. The locus shown in (2) of (B) is a little larger than the hole. This may be due to a small compliance in the experimental setup. Apart from this, the shape of each environment is truly reconstructed by the loci shown in (2) of (A) and (2) of (B). From this, it was verified that the finger fulfils its functions as a contact force and position sensor.

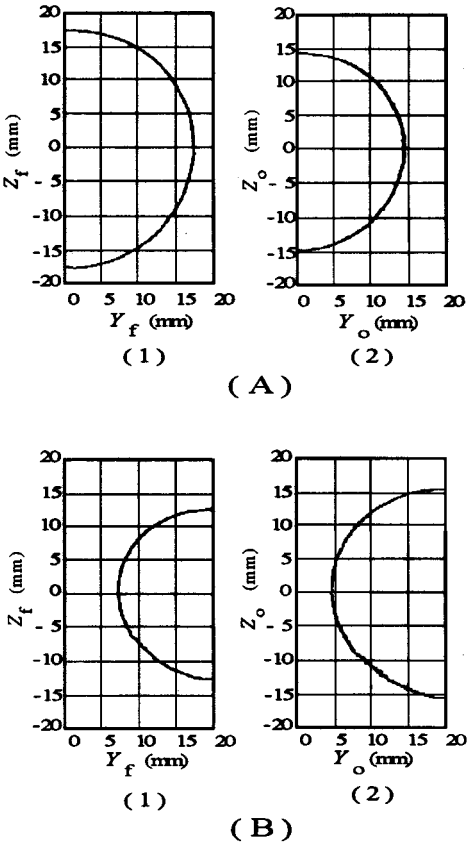

Figure 6. (A)-(1) Locus of the finger tracing the outer circumference of a half disk; (A)-(2) Reconstructed two-dimensional shape of the half disk; (B)-(1) Locus of the finger tracing the inner circumference of a semicircular hole; (B)-(2) Reconstructed two-dimensional shape of the semicircular hole

4 CONCLUSION

Because the output of a force sensor using quartz resonators is a frequency shift, it is insensitive to electrical noise, has a quick response, high sensitivity, high resolution and a wide bandwidth. A finger with four pairs of quartz resonators as a contact force and position sensor was proposed in order to apply quartz resonators for robot sensor applications. The performance of the sensor was verified experimentally. Sensing an environment was carried out using the finger. It was shown that quartz resonators can be utilized in a robot sensor.

ACKNOWLEDGMENT

The author would like to thank Japan Society for the Promotion of Science for supporting this work through Grant-in-Aid for Scientific Research.

REFERENCES

[1] S. Muraoka, R. Masuo, C. Maeda, Temperature dependence of force sensitivity of a quartz resonator used in a force sensor, ACTA IMEKO XII, Measurement of Force, Mass, Pressure, Flow and Vibration, (1991) 379 - 384
[2] S. Muraoka, Application of quartz resonator to grasping force sensor, New Measurement - Challenges and Visions, IXB, (1 997) 55 - 60
[3] S. Muraoka, Detection of grasping foree and slip using quartz resonators, Measurement of Improve the Quality of Life in the 21st Century - Measurement Helps to Coordinate Nature with Human Activities -, X-TC17, (1999) 165 -172

AUTHOR: S. MURAOKA, Osaka Institute of Technology, Department of mechanical engineering, 5-16-1, Ohmiya, Asahi-Ku, Osaka, 535-8585, Japan, Phone: Int +81 6 6954 4262, Fax: lnt +8l 6 6957 2134, E-mail: muraoka@med.oit.ac.jp